MATERIAL PROPERTIES OF EXISTING UNREINFORCED CLAY BRICK MASONRY BUILDINGS IN NEW ZEALAND

Nasser Almesfer[1], Dmytro Y. Dizhur[2], Ronald Lumantarna[3], Jason M. Ingham[4]

SUMMARY

The material properties of New Zealand's heritage clay brick unreinforced masonry (URM) buildings were investigated and are reported herein. Material data was collected from a total of 98 New Zealand clay brick URM buildings and a database was compiled that was comprised of various masonry material properties. The intention behind the reporting of information and data presented herein was to provide indicative values to the professional engineering community to aid as preliminary input when undertaking detailed building assessments for cases where in-situ testing and brick and mortar sample extraction are not feasible. The data presented is also used to support the relationships for URM material properties that have been recommended by the authors for incorporation into the next version of the NZSEE seismic assessment guidelines for URM buildings. Although researchers from Europe, USA, India and Australia have previously studied the material properties of clay brick unreinforced masonry, knowledge on New Zealand URM material properties was poor at the time the study commenced. Therefore, a research programme was undertaken that was focused on both in-situ testing and laboratory testing of samples extracted from existing New Zealand clay brick URM buildings.

INTRODUCTION

Unreinforced masonry (URM) buildings are generally New Zealand's oldest buildings, representing both a large and a significant component of the nation's architectural heritage. Whilst URM buildings are prevalent worldwide, New Zealand has the comparative advantage that our URM building stock was constructed over a short time frame spanning from about 1880 to 1935 and most buildings have a regular and widely repeated geometry and detailing that facilitates the development of seismic assessment guidelines that have the potential for a greater degree of accuracy than is possible in many other parts of the world where the URM building stock is far more diverse.

URM construction is evidently vulnerable to large magnitude earthquakes [1, 2, 3]. The most recent New Zealand examples of the vulnerability of URM buildings to earthquakes were the 4th September 2010 Darfield earthquake and the 22nd February 2011 Christchurch earthquake [4, 5, 6] where most URM buildings in the Christchurch area were severely damaged (see Figure 1), leading to fatalities. Today many URM buildings still exist in various parts of New Zealand and due to their likely poor earthquake performance, seismic assessment and retrofit of these remaining URM buildings will probably be required in most cases in order to avoid building demolition, recognising that these buildings not only represent a significant architectural heritage, but also occupy a significant proportion of the nation's building stock.

Figure 1: Damaged URM building resulting from the 2011 Christchurch earthquake.

Design practitioners have communicated the importance of obtaining better material data for URM buildings in order to improve the accuracy, and therefore the cost effectiveness of their seismic assessments, computer modelling, and retrofit designs. The study reported herein concentrated specifically on the material properties of pre-1950s New Zealand URM

[1] *Structural Engineer, EQ Struc Ltd*

[2] *Post-doctoral fellow, Department of Civil and Environmental Engineering, University of Auckland, Auckland, New Zealand*

[3] *National Sales Engineer, Reids Construction Systems Ltd*

[4] *Professor, Department of Civil and Environmental Engineering, University of Auckland, Auckland, New Zealand*

buildings that were constructed using solid, uncored clay bricks having approximate dimensions of 230 mm × 110 mm × 76 mm, and lime-based mortar (in alignment with Russell [7]). This construction type is still largely used in developing countries such as India and Indonesia [8, 9, 10, 11], and researchers from USA, Australia and Europe have previously studied the material properties of clay brick unreinforced masonry.

A clay brick unreinforced masonry assemblage has nonhomogeneous, inelastic and orthotropic material characteristics, whose properties are influenced by both the brick unit and mortar properties. Therefore, this study aimed to investigate the brick unit and mortar properties separately, and to then relate the brick unit and mortar properties to the masonry assemblage properties.

PAST STUDIES AND COMMON TEST METHODS TO DETERMINE URM MATERIAL PROPERTIES

Clay bricks

Clay bricks are a principal structural component of unreinforced clay brick masonry buildings, and researchers [10, 11, 12] have commonly used the clay brick compressive strength as a principal parameter to predict masonry compressive strength, which furthermore is the basis for estimating masonry Modulus of Elasticity and stress-strain behaviour [11]. However, the extraction of clay bricks from heritage URM buildings for compression testing is often prohibited due to the building's heritage significance. NZSEE [13] recommends the use of physical properties such as colour to classify clay bricks, which was shown by Lumantarna [14] to not be an appropriate basis for a brick classification scheme as there was no measured correlation between brick colour and brick compressive strength (see Figure 2). Overseas researchers [15, 16] have suggested the use of different techniques to determine the brick compressive strength, such as the Schmidt hammer test and the ultrasonic pulse velocity test.

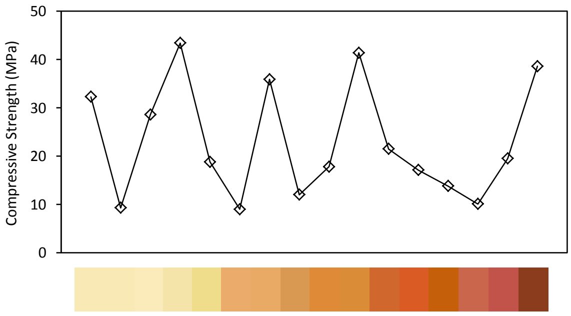

Figure 2: Brick compressive strength vs. visible colour plot.

Another non-destructive testing technique is the Mohs scratch test, which is used to estimate material properties based on the material's resistance to abrasion, and is associated with the Mohs hardness scale. Mohs numbers of 1 to 10 are used to rank minerals with distinct hardness, and the scratch number assigned to the tested sample is equal to the Mohs number of the mineral that scratches it [17]. The scratch test is principally similar to the abrasion test described by Shalabi *et al.* [18], where the resistance of one material against another material of a different hardness is tested. Shalabi *et al*. [18] also reported that there is a linear relationship between the compressive strength of rocks and their abrasion hardness. However, the feasibility of the above techniques to characterise New Zealand heritage clay bricks had not been rigorously verified prior to commencement of the reported study.

Mortar

The mortar compressive strength has also been used previously by a number of researchers [10, 11, 12] for the prediction of masonry compressive strength. However, mortar samples extracted from existing URM buildings are typically of an irregular shape, and thus these samples are not suitable for standardised compression testing. Procedures for the compression testing of irregular mortar samples have been studied by a number of authors [19, 20, 21] who have performed laboratory experiments and finite element modelling to investigate the influence that sample dimensions had on the measured value of the mortar compressive strength. Other authors have investigated procedures to estimate the mortar aggregate to binder ratio [22] and to predict the mineral constituents of mortar [23, 24, 25].

Masonry assemblage

The material properties of a masonry assemblage have typically been studied using a single leaf, stack bonded brick/mortar composite of a given brick-height (referred to as a "masonry prism"). Kaushik *et al.* [11] used laboratory-constructed masonry prisms to study the relationships between brick unit compressive strength, mortar compressive strength, masonry compressive strength, masonry compression stress-strain behaviour and masonry Modulus of Elasticity, whilst other authors [26, 27] used laboratory constructed masonry prisms to relate the brick unit, mortar and masonry compressive strengths to the masonry flexural bond strength and shear bond strength. However, it is noted that these studies mostly focused on newly made laboratory-constructed samples, and thus the applicability of these studies to New Zealand heritage URM required investigation.

Masonry compressive strength is one of the most important properties for the assessment and design of masonry elements [11]. However, compression testing of masonry prisms is not always practical, and therefore many researchers [9, 10, 11, 28, 29] have attempted to develop an empirical expression relating the brick unit, mortar and masonry compressive strengths in a form such as shown in Equation 1 [30]:

$$f'_m = K f'^{\alpha}_b \times f'^{\beta}_j \qquad (1)$$

where, K, α, and β are constants, and f'_b, f'_j and f'_m are the brick unit, mortar and masonry compressive strengths respectively. Eurocode 6 [30] recommends a range of K values, depending on the brick unit properties and the brick/mortar bond configuration, while prescribing α and β as 0.7 and 0.3 respectively. The value of β is lower than α, which indicates that the masonry compressive strength (f'_m) is influenced to a greater extent by the brick unit compressive strength (f'_b) than by the mortar compressive strength (f'_j). It is noted that the constants proposed by Eurocode 6 [30] are used to estimate the 5% lower characteristic compressive strength of masonry, instead of the mean compressive strength.

Modulus of Elasticity

The masonry Modulus of Elasticity (E_m) is commonly calculated as the chord modulus of the linear part of the masonry compression stress-strain curve, which is typically defined to be between 5% and 33% of the ultimate masonry compressive strength (f'_m) [1, 31]. The relationship between masonry compressive strength and Modulus of Elasticity can be expressed as:

$$E_m = kf'_m \quad (2)$$

where k is a constant that varies from one recommendation to another. The MSJC code [32] and FEMA 306 [33] from North America recommend that E_m is equal to $700f'_m$ for modern masonry and equal to $550f'_m$ for existing masonry respectively, whilst the Canadian masonry code [34] suggests a slightly higher value of $E_m = 850\,f'_m$ for modern masonry.

Masonry bond strength

Several studies have been previously conducted to investigate masonry bond properties. The brick/mortar bond development is effectively a mechanical process that is influenced by binder hydration occurring at the brick surface and in the brick unit pores [35, 36, 37]. Grenley [38] investigated various brick/mortar combinations and found that the masonry flexural bond, tensile bond and compressive strengths generally increased with increasing brick unit and mortar compressive strengths. The masonry bond-compressive strength relationships that were obtained for the various combinations showed strong correlations, although the influence that mortar compressive strength had on the masonry bond strength could not be neglected. Samarasinghe and Lawrence [39] performed shear tests on masonry triplets replicating new masonry construction and observed that masonry prisms that were constructed using pre-wetted brick units had higher bed joint shear strengths than those constructed using dry or completely saturated brick units. These researchers also observed that the bed joint shear strength increased with increasing mortar compressive strength.

The brick/mortar bond failure of masonry prisms when subjected to bond wrench and shear bond tests can be classified as follows [26, 40, 41]:

- Type A: Failure at one brick/mortar interface;
- Type B: Failure at both brick/mortar interfaces;
- Type C: Failure within the mortar joint;
- Type D: Failure within the brick unit;
- Type E: Combination of failure within the brick unit and mortar joint.

Venkatarama Reddy and Gupta [41] observed four different types of failure (types A, C, D and E) for their experiments. Failure type E was the most common type observed, whilst failure types C and D generally occurred when weak mortar and weak block units respectively were used. Failure type A was exhibited by prisms that were constructed using moderately strong cement-soil blocks. Sarangapani *et al.* [26] did not observe failure type C when testing masonry prisms, whereas failure type D and a combination of failure types A and D were frequently observed for prisms constructed using weak brick units and strong mortar. These researchers also reported that failure type A mostly occurred when the brick/mortar interface bond strength was lower than the mortar joint flexural strength, and therefore this failure type was exhibited by almost all prisms that were constructed without bond enhancement.

TEST PROGRAM

Vintage clay bricks and irregular mortar samples were extracted from existing New Zealand URM buildings, and were subjected to a series of non-destructive tests before being tested in compression. The relationships between the non-destructive test results and the clay brick and mortar compressive strengths were studied, and non-destructive testing techniques that were most suitable for estimating clay brick and mortar compressive strengths in-situ were proposed. The compressive strength and compressive stiffness of masonry were studied using masonry prisms (see Figure 3) that were both extracted from existing buildings and were constructed in the laboratory. Empirical relationships relating the brick unit, mortar and masonry compressive strengths as well as relating the masonry compressive strength to the masonry Modulus of Elasticity were derived.

Figure 3: Masonry prism with displacement gauge.

Finally, the flexural bond strength and shear bond strength of masonry were studied using field extracted and laboratory constructed masonry prisms. Empirical relationships relating the mortar compressive strength to the flexural bond strength and to the bed joint cohesion were derived.

METHODOLOGY

The compressive strength of the brick units that were used in the construction of each prism combination was determined following the half brick compression test ASTM C 67 - 03a [42], which involves cutting extracted brick units into halves and capping these half bricks prior to compression testing using gypsum plaster for the capping material (see Figure 4). The purpose of this investigation was to correlate the measured brick compressive strength using a standard test to the measured compressive strength of the prism, again using a standard test.

Figure 4: Gypsum plaster capping (left, and brick compression testing (right).

Irregular mortar samples were extracted from each field site and carefully cut in the laboratory to form rectangular test pieces, then capped using gypsum plaster and tested in compression following the procedure reported by Lumantarna [14], (see Figure 5).

The method to determine mortar compressive strength is detailed in ASTM C 109-08 [43]. This method involves testing of 50 mm cube mortar samples, which generally are not attainable in existing buildings as most mortar joints are only

12 to 18 mm thick. Consequently, irregular mortar samples were cut into approximately cubical sizes with two parallel sides (top and bottom). The height of the mortar samples exceeded 15 mm in order to satisfactorily maintain the proportion between sample size and the maximum aggregate size. The prepared samples were then capped using gypsum plaster to ensure a uniform stress distribution and tested in compression [20].

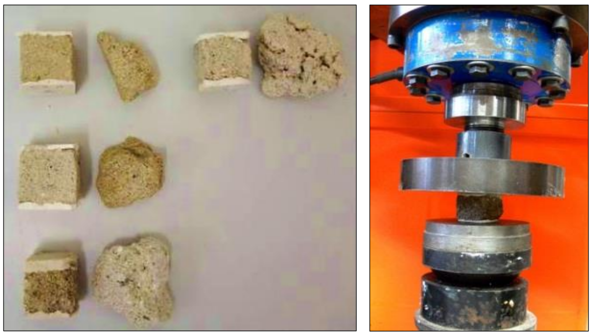

***Figure 5:** Irregular mortar samples (left) and mortar compression test (right).*

The height to least lateral dimension (h/t) ratio of the mortar samples was measured and used to determine the mortar compressive strength correction factors by interpolation of the data presented in Table 1. The compression test result was then divided by the corresponding correction factors listed in Table 1. Refer to Lumantarna [14] for further details regarding the correction factors and the influence of height to thickness ratio on mortar compressive strength.

***Table 1:** Height to thickness ratio correction factor for mortar compressive strength*

***h/t* ratio**	0.6	0.7	0.8	0.9	1.0	1.1	1.2
Correction factor	1.3	1.225	1.15	1.075	1.00	0.925	0.85

For the laboratory constructed prisms, varying mortar mix proportions were selected to simulate a wide range of mortar properties, and the materials used in the mortar were ordinary Portland cement, hydrated lime and river sand. Most of the mortar mix proportions chosen were based on the proportions recommended in ASTM C 270 - 08a [43] and the typical material proportions for New Zealand historic mortar as reported in NZSEE [13], except for mortar grades B and E, which were approximated by the mason that assisted in the sample construction process. The water/cement ratio of each mortar grade was kept constant to maintain between-batch consistency. It is noted that these mortar cubes were prepared simultaneously with the laboratory constructed prisms. The compressive strength of each mortar grade was determined using 50 mm mortar cubes that were prepared as prescribed in ASTM C 109 - 08 [43]. After approximately 28 days of curing at room temperature (20 ± 5º C) these mortar cubes were tested in compression following ASTM C 109 - 08 [43].

The bond wrench test AS 3700-2001 [44] was adopted for both in-situ and laboratory applications due to its greater portability in comparison to the ASTM C 1072 - 00a [45] test setup, and therefore the bond wrench test was more suitable for in-situ testing. The bond wrench arm was constructed as stipulated in AS 3700-2001 [44], with a hook connector installed at the end of the bond wrench arm. An empty container was attached to the hook and then gradually filled using sand to apply bending stresses to the mortar joint until flexural bond failure occurred (see Figure 6). The weight of the bucket and sand was measured to the nearest 0.01 gram and used to calculate the flexural bond failure stress.

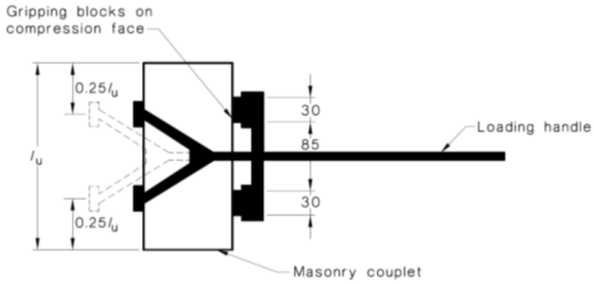

(a) Plan view

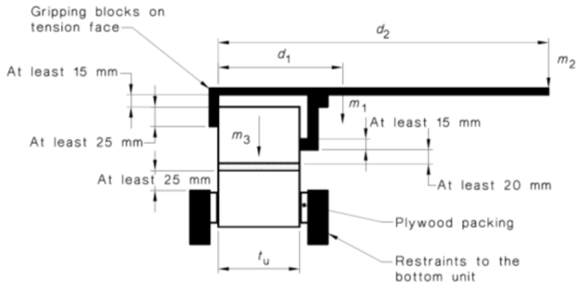

(b) Elevation view

***Figure 6:** Flexural bond test-setup (AS 3700-2001).*

The in-situ shear test ASTM C 1531 - 03 [46] and the triplet shear test Rilem TC 127-MS.B.4 [47] were adopted for on-site and laboratory shear bond testing respectively, with the majority of tests being performed using the in-situ shear test. The in-situ shear tests were performed without flat jacks, and the triplet shear tests were performed whilst subjected to different levels of axial pre-compression load. The hydraulic jack was loaded using a pressure controlled hydraulic pump and a displacement gauge was attached on the wall face adjacent to the vertical cut joint, to identify when bed-joint sliding failure occurred (see Figure 7). It was also noted that the contribution of collar joints was not considered in the bed joint shear strength calculation as the collar joints were mostly poorly laid, and therefore their contribution to the bed joint shear strength was minimal.

***Figure 7:** In-situ shear test.*

For the triplet shear test, prisms were placed between two steel plates that were interconnected using four steel rods. The axial pre-compression load was applied by tightening the nuts at the ends of the steel rods and the value of the pre-compression load was recorded using a load cell. The sample was prepared such that the middle course of the prisms consisted of a full brick unit (see Figure 8).

Figure 8: Laboratory shear triplet.

The triplet shear tests were performed whilst being subjected to axial pre-compression stresses of 0.2 MPa, 0.4 MPa and 0.6 MPa. The shear strength of the mortar joints can be represented by the Mohr-Coulomb friction law as per Equation (3) [42, 47, 48]:

$$\tau = c + \mu N \quad (3)$$

where τ = shear stress at a given axial compression, c = shear stress at zero axial compression (cohesion), μ = coefficient of friction, and N = axial compression stress. Therefore, the mortar bed joint cohesion could be derived because the triplet shear tests were performed at different levels of axial pre-compression load.

Source of extracted samples

The brick and mortar samples were extracted from 98 buildings (referred to as field sites) which were constructed between 1881 and the 1940s, which coincides with the time period during which URM construction was popular in New Zealand. Although variability in the constituent material properties amongst URM buildings is expected, these field sites are deemed to be representative of the majority of New Zealand URM buildings. Figure 9 below shows the locations of the field sites. Refer to Appendix A for more details on each field site.

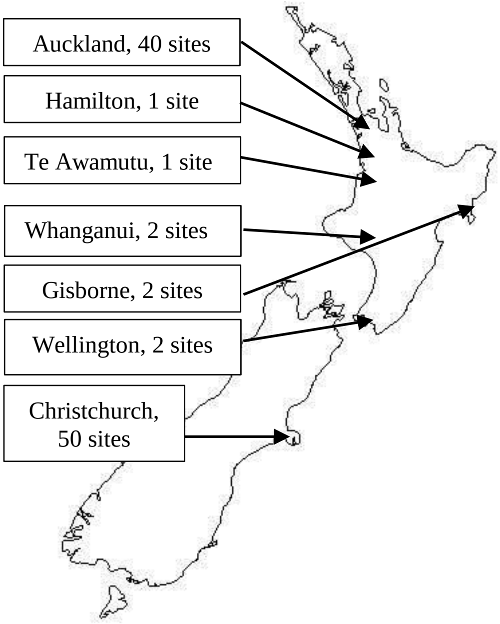

***Figure 9:** Map of New Zealand showing the location of field sites.*

TEST RESULTS AND DISCUSSION

Mohs scratch test - brick

A statistical analysis of the relationship between brick unit compressive strength and Mohs scratch number was performed using the R software package [49]. The brick unit compressive strength-Mohs scratch number relationship was expressed using the box and whisker plots shown in Figure 10, which were calculated according to Peck *et al*. [50]. It is noted that the group median was used to express each brick category (each box and whisker plot) as median is less influenced by data extremes than is the mean, and therefore was considered to be suitable when dealing with a large data population. Figure 10 shows that the median compressive strengths of brick units with scratch numbers of 2.5, 3.0 and 4.0 were 13.3 MPa, 27.5 MPa and 37.2 MPa, respectively. It was found that an increase in brick unit compressive strength generally correlated with an increased Mohs scratch number. The Mohs scratch numbers were generally consistent within each brick group, except for some brick groups where slight variability in the numbers was obtained. The majority of the samples were scratched using an aluminium pick (Mohs scratch number 2.5, 89 samples), whilst there were 41 and 27 samples that were scratched using a copper coin (Mohs scratch number 3.0) and an iron nail (Mohs scratch number 4.0) respectively. The brick surface abrasion resistance may be affected by weathering, and hence it is important to consider scraping off the potentially weathered surface of the brick prior to performing the scratch test in order to obtain a more accurate result.

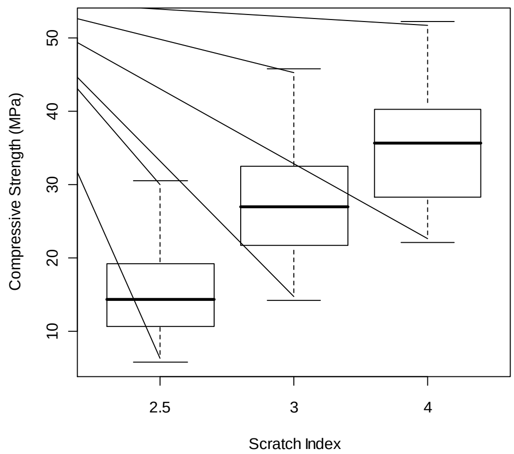

***Figure 10:** Relationship between brick unit compressive strength and Mohs scratch number (157 data considered).*

The data presented in Figure 10 consisted of a data set from earlier studies published by Lumantarna [14], whereas a larger brick compressive strength data set is presented in Figure 11 (which also includes all the data from Figure 10), along with the relative frequency of strength bands. Based on Figure 10 a scratch index of 2.5 would correlate with an anticipated upper limit of brick unit compressive strength of approximately 30 MPa, and therefore potentially include up to 80% of the compressive strength data set shown in Figure 11. This observation illustrates the inherent uncertainty and potential inaccuracy associated with use of the scratch test to forecast compressive strength, particularly for a scratch index of 2.5, and hence it is recommended that engineers undertake a sensitivity analysis to consider what effect a high or low brick compressive strength may have on their assessments. The Mohs scratch test should only be performed if extraction of brick samples from the building is not possible.

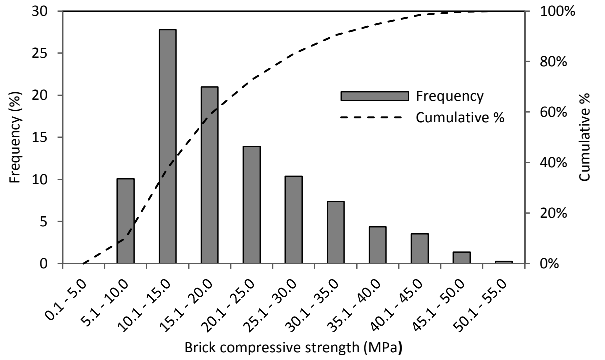

Figure 11: Brick compressive strength frequency distribution (367 data considered).

Brick unit Modulus of Rupture

The brick unit Modulus of Rupture (MoR) and compressive strengths of 8 different brick groups are shown in Figure 12. The brick unit Modulus of Rupture strength generally increased with increasing brick unit compressive strength. The average brick unit compressive strength ranged between 10.0 MPa and 28.9 MPa, whilst the average brick unit Modulus of Rupture strength varied from 0.9 MPa to 3.8 MPa. The Coefficient of Variation (CoV) values of the Modulus of Rupture strength were generally higher than those of the brick unit compressive strength (CoV *MoR* ranging from 0.15 to 0.39 and CoV f'_b ranging between 0.17 and 0.30). Figure 12 illustrates the brick unit Modulus of Rupture strength-compressive strength relationship. It was established that the brick unit Modulus of Rupture strength can be satisfactorily equated to:

$$MoR = 0.12\, f'_b \tag{4}$$

which is similar to the $0.10f'_b$ value recommended in NZSEE [13], and the associated coefficient of determination (R^2) value of 72% was deemed to be satisfactory, especially when considering the variability of New Zealand vintage solid clay bricks.

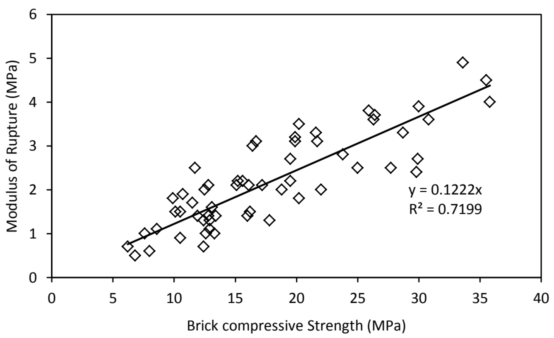

Figure 12: Relationship between brick Modulus of Rupture strength and brick compressive strength.

Mohs scratch test - mortar

The normalised mortar compressive strength-Mohs scratch number relationship was expressed using the box and whisker plots shown in Figure 13, which were again calculated according to Peck *et al.* [50]. Similar to that for clay bricks, the group median was used to express each mortar category (each box and whisker plot) as median is less influenced by data extremes than is the mean, and therefore was considered to be suitable when dealing with a large data population. Figure 13 shows that the median normalised compressive strengths of mortar samples having scratch numbers of 1.5, 2.0, and 2.5 were 1.4 MPa, 5.5 MPa, and 7.4 MPa, respectively.

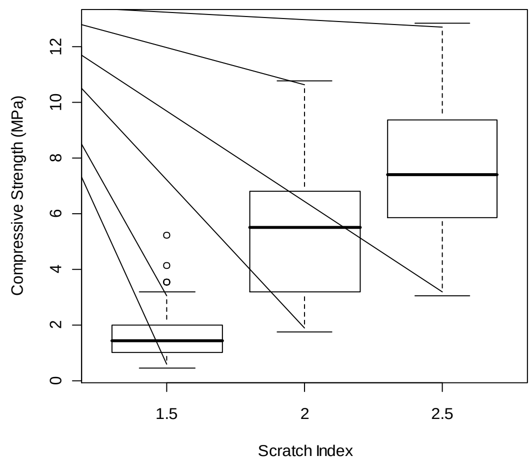

Figure 13: Relationship between mortar compressive strength and Mohs scratch number.

It was found that the normalised mortar compressive strength generally increased with an increase in the Mohs scratch number. The Mohs scratch numbers were generally consistent within each mortar group, except for some mortar groups where slight variability in the scratch numbers was observed. The samples were scratched easily with a fingernail (Mohs scratch number 1.5, 223 samples), whilst there were 92 and 42 samples that were scratched with a fingernail (Mohs scratch number 2.0) and an aluminium pick (Mohs scratch number 2.5) respectively.

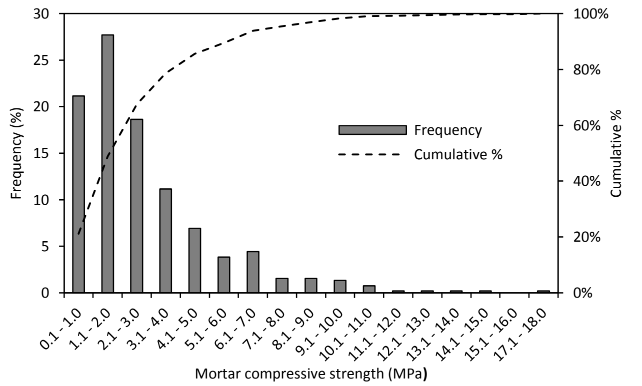

Figure 14: Mortar compressive strength frequency distribution (357 data considered).

The Kruskal - Wallis test [51] revealed that each mortar category originated from samples which had a distinct median, suggesting that the modified Mohs scratch test is an adequate technique to categorise mortar samples according to their compressive strengths. However, each Mohs scratch number represents a wide mortar compressive strength range as supported by Figure 14, where a scratch index of 1.5 (from Figure 13 potentially having an upper mortar compressive strength of approximately 3.0 MPa) includes up to 70% of the mortar compressive strength data set. Consequently this testing technique should be reserved for cases where there is no budget available for extraction of samples, or when sample extraction from heritage URM buildings is not permitted. If this testing technique is used, the scratch test needs to be undertaken at a suitable mortar depth due to possible mortar repointing.

Data from Figure 14 is represented in Figure 15 with higher resolution strength bands, indicating that the most frequently encountered mortar strengths ranged between 0.6 MPa and 1.5 MPa, with approximately 40% of all samples having compressive strengths of less than 1.5 MPa.

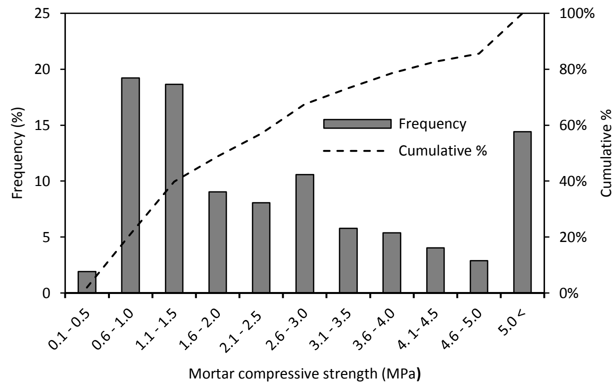

Figure 15: Mortar compressive strength frequency distribution (2); (357 data considered).

Prediction of masonry compressive strength

An expression relating the brick unit, mortar and masonry compressive strengths was derived to enable prediction of the compressive strength of existing URM buildings using only the brick unit and mortar compressive strengths, so that expensive and time consuming prism compression tests can be avoided. In general, the masonry compressive strength increased with increasing brick unit and mortar compressive strengths. The field extracted sample test results were combined with those of the laboratory constructed samples, and a non-linear regression analysis was performed to determine the relationships between f'_b, f'_j and f'_m for the combined data set, allowing the resemblance of the laboratory constructed samples to the field extracted samples to be assessed. A three dimensional plot relating f'_b, f'_j and f'_m of the combined database was generated using DataFit 9.0 [52] as illustrated in Figure 16. It was shown that the f'_b, f'_j and f'_m relationships of the laboratory constructed samples converged with those of the field extracted samples. The surface plot in Figure 16 represents the prediction of masonry compressive strength for different brick unit and mortar properties. A predictive equation relating f'_b, f'_j and f'_m in the form of the Eurocode 6 expression [30] was derived, and constants K, α, and β were found to be 0.75, 0.75 and 0.31, respectively, as show in equation 5.

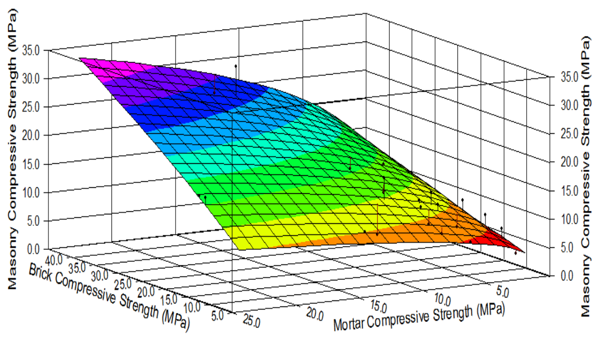

Figure 16: Three-dimensional plot relating f'_b, f'_j and f'_m.

$$f'_m = 0.75 f'^{0.75}_b \times f'^{0.31}_j \qquad (5)$$

In agreement with previous studies [10, 11, 12, 30], the β value (0.31) was found to be lower than the α value (0.75), which implied that the mortar compressive strength had less influence on the masonry compressive strength than did the brick unit compressive strength. An R^2 value of 87% was obtained, which was deemed to be satisfactory, especially when considering that this equation suited both field extracted and laboratory constructed masonry.

Prediction of masonry Modulus of Elasticity

As masonry Modulus of Elasticity is an important property for linear and non-linear structural analysis, a predictive expression relating the masonry Modulus of Elasticity to the masonry compressive strength was derived. The masonry Modulus of Elasticity generally increased with increasing masonry compressive strength. The masonry Modulus of Elasticity-compressive strength relationship of the combined dataset for both the field extracted and the laboratory constructed prisms is illustrated in Figure 17, showing good agreement between the two separate data sets. For the combined dataset, E_m could be satisfactorily determined from equation 6 below. This expression had an R^2 value of 76%, which was deemed to satisfactorily predict the masonry Modulus of Elasticity.

$$E_m = 294 f'_m \qquad (6)$$

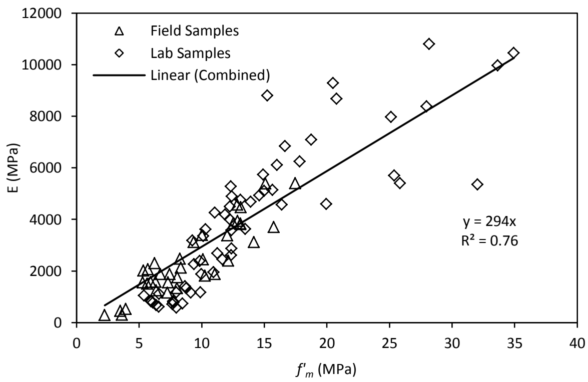

Figure 17: Relationship between masonry compressive strength and masonry Modulus of Elasticity.

When compared with the k values recommended elsewhere, the derived k value of 294 that is presented in equation 6 for New Zealand historic clay brick masonry was notably low, although this derived value was within the range observed by Drysdale *et al.* [1] and Kaushik *et al.* [11]. It is also noted that one important reason for the derived value being lower than is customarily recommended was that the masonry Modulus of Elasticity was intentionally calculated using the stress and strain ordinates at $0.05f'_m$ and $0.70f'_m$ instead of those located at $0.05f'_m$ and $0.33f'_m$ as used by previous researchers. This adopted calculation method generated a stiffness value appropriately reflecting the likely stiffness as appropriate for linear or non-linear analysis of the in-plane response of masonry walls or piers when the true stress-strain relationship is approximated by an elastic-perfectly plastic relationship, and therefore although the derived E_m values were low, they were thought to be representative for use in both linear and non-linear seismic analyses.

Modulus of Elasticity values were also established from flat jack tests undertaken in accordance with ASTM C 1197 – 04, and these tests have repeatedly led to higher values of Modulus of Elasticity than is proposed above. However, it is noted that in general these flat jack tests were undertaken for lower levels of peak stress, when compared to the crushing of masonry prisms, and hence a higher Modulus of Elasticity would be expected for testing to a reduced stress level.

Higher Modulus of Elasticity values were particularly noticeable for masonry having a higher compressive strength. It is recommended that a sensitivity study be conducted on the effects that the adopted Modulus of Elasticity has on the outcome of the building seismic assessment and that on-site testing be conducted where uncertainty in the value of masonry Modulus of Elasticity has a significant influence on the determination.

Flexural bond strength

A minimum of three bond wrench couplet samples were tested for each brick/mortar combination, with most prisms exhibiting a flexural bond failure within the mortar joint (failure type C). It was concluded that these bond failures within the mortar joints occurred because the heritage buildings investigated in this experimental programme were constructed using lime-rich mortars, and therefore the mortar did not have sufficient strength to resist the applied tensile force. Furthermore, it was found that samples which exhibited brick/mortar interface bond failure (failure type A) had lower flexural bond strengths than those which exhibited failure type C. It was thought that samples that exhibited brick/mortar interface bond failure were either disturbed during their preparation or were not constructed properly (referred to as "lesser" samples), and thus resulting in low flexural bond strengths being recorded.

The average flexural bond strength of the field samples ranged from 0.031 MPa to 0.345 MPa. The variability in the bond wrench test results (CoV between 0.11 and 0.33) was thought to be reasonable when considering the irregular nature of URM construction. Figure 18 shows that the average masonry flexural bond strength increased with increasing average mortar compressive strength. Figure 18 also shows that the masonry flexural bond strength, f'_{fb}, can be satisfactorily equated to:

$$f'_{fb} = 0.03 f'_j \quad (7)$$

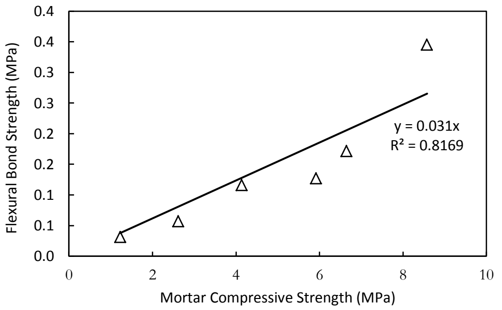

Figure 18: Flexural bond strength-mortar compressive strength relationship.

Bed-joint cohesion

Figure 19 illustrates the relationship between mortar bed joint cohesion and average mortar compressive strength. It is shown that the mortar bed joint cohesion, *c*, was particularly variable, especially for cohesion values obtained by EQ Struc Ltd using the in-situ shear test procedure prescribed in ASTM C 1531 - 03 [46], whereas the cohesion test data obtained by Lumantarna [14] were based on the triplet shear test arrangement in a laboratory [47]. All samples considered in the derivation of the relationship between cohesion and mortar compressive strength had exhibited shear bond failures within their mortar joints.

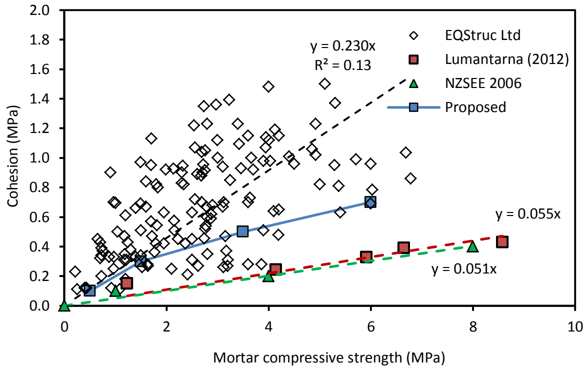

Figure 19: Cohesion-mortar compressive strength relationship.

As indicated in Figure 19, the cohesion to mortar compressive strength relationships proposed by Lumantarna [14] and by NZSEE [13] are similar. However, the cohesion results obtained from the significantly larger dataset compiled by EQ STRUC Ltd are notably higher and all results were greater than the values proposed by Lumantarna [14] and NZSEE [13].

Table 2: Proposed cohesion values

Mortar hardness	Mortar description	Mortar compressive strength (MPa)	Cohesion (MPa)
Very soft	Raked out by finger pressure	0-1	0.1
Soft	Scratches easily with finger nails	1-2	0.3
Medium	Scratches with finger nails	2-5	0.5
Hard	Scratches using aluminium pick	5-7	0.7
Very hard	Does not scratch with above tools	To be established from testing	

It is clear that the cohesion values previously proposed are potentially too low, which may have significant implications when assessing the capacity of URM walls, and in particular when seeking to establish the critical in-plane capacity of individual piers for different deformation modes. Hence, cohesion values for use in seismic assessment have been proposed as shown in Figure 19. The proposed values should be adopted for preliminary reference only, or when in-situ bed joint shear testing is strictly not permitted. The cohesion values proposed in Figure 19 and presented in Table 2 were based upon grouping all cohesion data shown in Figure 19 into bands of mortar hardness (which was then correlated with mortar compressive strength, see Table 2), and then for all data within that band establishing the cohesion value corresponding to mean minus one standard deviation. Also, it is noted that the dashed line in Figure 19 represents the best fit for the entire data set, although care should be exercised if the mean value is to be considered as then there is a significant likelihood that the true cohesion value will be significantly over-estimated.

CONCLUSIONS

The research reported herein was conducted with the aim to develop a comprehensive data set to inform potential revision of the unreinforced masonry material property recommendations prescribed in NZSEE [13]. To achieve this aim, an experimental programme that focused mainly on the testing of clay bricks, mortar and masonry prisms that were extracted from New Zealand heritage URM buildings was undertaken. Further data that greatly expanded the complete data set was provided by EQ Struc limited, derived from in-situ testing of URM buildings as part of seismic assessments.

- It was found that an increase in brick unit compressive strength generally correlated with an increased Mohs scratch number. However, each Mohs scratch number represents a wide range of brick unit compressive strength, and therefore it is recommended that this testing technique be reserved for cases where destructive testing is not permitted.
- The brick unit Modulus of Rupture strength generally increased with increasing brick unit compressive strength, and can be equated to $0.12f'_b$.
- It was found that an increase in the normalised mortar compressive strength generally led to an increase in the Mohs scratch number. It was also suggested that this testing technique be reserved for cases where sample extraction is not permitted.
- The masonry compressive strength was found to increase with increasing brick unit and mortar compressive strengths.
- When the data sets for the field extracted and the laboratory constructed sample test results were combined, E_m was equated to $294f'_m$. E_m attained from in-situ flat jack tests has repeatedly led to higher values, perhaps due to loading to lower stress levels. Higher E_m values were particularly noticeable for masonry with higher values of f'_m. It is recommended that a sensitivity study be conducted on the effects of E_m on the outcome of the building assessment and that on-site testing be conducted if deemed necessary.
- The masonry flexural bond strength was related to the mortar compressive strength and equated to $0.03f'_j$.
- Bed joint cohesion was related to the mortar compressive strength, and cohesion values for specific ranges of mortar compressive strength have been proposed for the purposes of preliminary building assessment.

The above recommendations are based on a limited number of samples with highly variable results and are not intended as a substitute to detailed material investigation and in-situ testing. It is always preferable to perform detailed material investigations of URM buildings, and values suggested herein should be adopted only for preliminary reference or when in-situ testing and material sample extraction is strictly not permitted. When future opportunities for sample extraction arise, it is recommended that both compression tests and modified Mohs scratch tests on heritage clay bricks and mortar be performed to further populate the brick unit and mortar scratch test database. The brick unit Modulus of Rupture strength and Modulus of Elasticity database can also be enriched by performing Modulus of Rupture tests and half brick compression tests whilst incorporating displacement gauges. It is thought that with an expanded database of material properties derived from samples extracted from existing URM buildings, predictive equations and numerical models for seismic assessment and retrofit design can be further refined in future.

ACKNOWLEDGEMENTS

The authors would like to thank EQ Struc Ltd for their help in providing material testing data. Funding for this study was provided by the Foundation for Research, Science and Technology and the New Zealand Natural Hazards Research Platform.

REFERENCES

1 Drysdale, R., Hamid, A., Baker, L. (1999). 'Masonry Structures: Behaviour and Design', *The Masonry Society*, Boulder, Colorado, United States.

2 Megget, L. (2006). 'From brittle to ductile: 75 years of seismic design in New Zealand', *Bulletin of The New Zealand Society for Earthquake Engineering*, **39**(3): 158-169.

3 Paulay, T., Priestley, M.J.N. (1992). 'Seismic design of reinforced concrete and masonry buildings', *John Wiley & Sons*, New York, United States.

4 Moon, L., Dizhur, D., Senaldi, I., Derakhshan, H., Griffith, M., Magenes, G., Ingham, J. (2014). 'The demise of the URM building stock in Christchurch during the 2010–2011 Canterbury earthquake sequence', *Earthquake Spectra*, **30**(1): 253-276.

5 Dizhur, D., Ingham, J. M., Moon, L., Griffith, M.C., Schultz, A., Senaldi, I., Magenes, G., Dickie, J., Lissel, S., Centeno, J., Ventura, C., Leite, J., Lourenco, P. (2011). 'Performance of masonry buildings and churches in the 22 February 2011 Christchurch earthquake', *Bulletin of New Zealand Society for Earthquake Engineering*, **44**(4): 279-297.

6 Dizhur, D., Ismail, N., Knox, C. Lumantarna, R. Ingham, J.M. (2010). 'Performance of unreinforced and retrofitted masonry buildings during the 2010 Darfield earthquake', *Bulletin of the New Zealand Society for Earthquake Engineering*, **43**(4): 321-339.

7 Russell, A. (2010). 'Characterisation and seismic assessment of unreinforced masonry buildings', Doctoral Dissertation, The University of Auckland, Auckland, New Zealand.

8 Basoenondo, E.A. (2008). 'Lateral load response of Cikarang brickwall structures: An experimental study', Doctoral Dissertation, Queensland University of Technology, Brisbane, Australia.

9 Deodhar, S.V. (2000). 'Strength of brick masonry prisms in compression', *Journal of the Institution of Engineers* (India), **81**(3): 133-137.

10 Gumaste, K.S., Nanjunda Rao, K.S., Venkatarama Reddy, B.V., Jagadish, K.S. (2006). 'Strength and elasticity of brick masonry prisms and wallettes under compression', *Materials and Structures*, **40**(2): 241-253.

11 Kaushik, H. B., Rai, D. C., Jain, S. K. (2007a). 'Stress-strain characteristics of clay brick masonry under uniaxial compression', *Journal of Materials in Civil Engineering*, **19**(9): 728-738.

12 Darayatnam, P. (1987). 'Brick and reinforced brick structures', Oxford and IBH, New Delhi, India.

13 NZSEE (2006). ‘Assessment and improvement of the structural performance of buildings in earthquakes’, *New Zealand Society for Earthquake Engineering*, Wellington, New Zealand.

14 Lumantarna, R. (2012). ‘Material characterisation of New Zealand's clay brick unreinforced masonry buildings’, Doctoral Dissertation, The University of Auckland, Auckland, New Zealand.

15 Brozovsky, J., Zach, J. (2007). ‘Non-destructive testing of solid brick compression strength in structures’, IV Conferencia Panamericana de END, Buenos Aires, Argentina, October.

16 Brozovsky, J., Zach, J., Brozovsky Jr., J. (2008). ‘Determining the strength of solid burnt bricks in historical structures’, 9th International Conference on NDT of Art, Jerusalem, Israel 25 -30 May.

17 Tabor, D. (1956). ‘The physical meaning of indentation and scratch hardness’, *British Journal of Applied Physics*, **7**(5): 159-166.

18 Shalabi, F.I., Cording, E.J., Al-Hattamleh, O.H. (2007). ‘Estimation of rock engineering properties using hardness tests’, *Engineering Geology*, **90**(3-4): 138-147.

19 Magalhães, A., Veiga, R. (2009). ‘Physical and mechanical characterisation of historic mortars: Application to the evaluation of the state of conservation’, *Materiales de Construccion*, **59**(295): 61-77.

20 Válek, J., Veiga, R. (2005). ‘Characterisation of mechanical properties of historic mortars - testing of irregular samples’, Structural Studies, Repairs and Maintenance of Heritage Architecture XI, Malta, 22 -24 June.

21 Drdácký, M., Mašín, D., Mekonone, M.D., Slížková, Z. (2008). ‘Compression tests on non-standard historic mortar specimens’, Historical Mortar Conference, Lisbon, Portugal, 24 -26 September.

22 Biggs, D., Forsberg, T. (2001). ‘Field techniques for mortar replication’, 9th Canadian Masonry Symposium, Fredericton, Canada, June.

23 Moriconi, G., Castellano, M.G., Collepardi, M. (1994). ‘Mortar deterioration of the masonry walls in historic buildings. A case history: Vanvitelli's Mole in Ancona’, *Materials and Structures*, **27**(7): 408-414.

24 Moropoulou, A., Bakolas, A., Bisbikou, K. (1995). ‘Characterization of ancient, byzantine and later historic mortars by thermal and X-ray diffraction techniques’, *Thermochimica Acta*, 269-270: 779-795.

25 Sabbioni, C., Zappia, G., Riontino, C., Blanco-Varela, M.T., Aguilera, J., Puertas, F., Van Balen, K., Toumbakari, E.E. (2001). ‘Atmospheric deterioration of ancient and modern hydraulic mortars’, *Atmospheric Environment*, **35**(3): 539-548.

26 Sarangapani, G., Venkatarama Reddy, B.V., Jagadish, K.S. (2005). ‘Brick-mortar bond and masonry compressive strength’, *Journal of Materials in Civil Engineering*, **17**(2): 229-237.

27 Venu Madhava Rao, K., Venkatarama Reddy, B. V., Jagadish, K. S. (1996). ‘Flexural bond strength of masonry using various blocks and mortars’, *Materials and Structures*, **29**(2): 119-124.

28 Kaushik, H. B., Rai, D. C., Jain, S. K. (2007b). ‘Uniaxial compressive stress-strain model for clay brick masonry’, *Current Science*, **92**(4): 497-501.

29 Ispir, M., Demir, C., Ilki, A., Kumbasar, N. (2010). ‘Material characterization of the historical unreinforced masonry Akaretler row houses in Istanbul’, *Journal of Materials in Civil Engineering*, **22**(7): 702-713.

30 CEN (2005). ‘Eurocode 6: Design of masonry structures -Part 1-1: General rules for reinforced and unreinforced masonry structures’, EN 1996-1-1:2005, European Committee for Standardization, Brussels, Belgium.

31 ASTM (2003). ‘Standard test method for compressive strength of masonry prisms’, C 1314-03b, ASTM International, Pennsylvania, United States.

32 MSJC (2002). ‘Building code requirements for masonry structures, ACI 530-02/ASCE 5-02/TMS 402-02’, America Concrete Institute, Structural Engineering Institute of the American Society of Civil Engineers, The Masonry Society, Detroit, Michigan, United States.

33 FEMA (1999). ‘Evaluation of earthquake damaged concrete and masonry wall buildings, basic procedures manual, ATC-43’, FEMA 306, *Federal Emergency Management Agency*, California, United States.

34 CSA (2004). ‘Design of masonry structures, S304.1’, Canadian Standards Association, Ontario, Canada.

35 Groot, C. (1993). ‘Effects of water on mortar brick bond’, Doctoral Dissertation, University of Delft, Delft, Netherlands.

36 Lawrence, S. J., Cao, H. T. (1987). ‘An experimental study of the interface between brick and mortar’, Proc., The 4th North American Masonry Conference, Los Angeles, California, United States, August, 1-14.

37 Sugo, H. O., Page, A. W., Lawrence, S. J. (2001). ‘The development of mortar/unit bond’, The 9th Canadian Masonry Symposium, Fredericton, New Brunswick, Canada, 4 - 6 June.

38 Grenley, D. G. (1969). ‘Study of the effect of certain modified mortars on compressive strength and flexural strength of masonry’, Designing, engineering, and constructing with Masonry Products, F. B. Johnson, ed., *Gulf Publishing Company*, Houston, United States, 28-33.

39 Samarasinghe, W., Lawrence, S. J. (1992). ‘Effect of high suction rate in low strength bricks on brick mortar bond’, Proc., The 4th International Seminar on Structural Masonry for Developing Countries, Madras, India, December, 43-50.

40 Pavia, S., Hanley, R. (2010). ‘Flexural bond strength of natural hydraulic lime mortar and clay brick’, *Materials and Structures*, **43**(7): 913-922.

41 Venkatarama Reddy, B. V. and Gupta, A. (2006). ‘Tensile bond strength of soil cement block masonry couplets using cement-soil mortars’, *Journal of Materials in Civil Engineering*, **18**(1): 36-45.

42 ASTM (2003a). ‘Standard test methods for sampling and testing brick and structural clay tile’, C 67 - 03a, ASTM International, Pennsylvania, United States.

43 ASTM (2008a). ‘Standard specification for mortar for unit masonry’, C 270 - 08a, ASTM International, Pennsylvania, United States.

44 Standards Australia (2001). ‘Appendix D: Method of test for flexural strength’, AS 3700 - 2001, Standards Australia, Homebush, New South Wales, Australia.

45 ASTM (2000). ‘Standard test method for measurement of masonry flexural bond strength’, C 1072 -00a, ASTM International, Pennsylvania, United States.

46 ASTM (2003b). ‘Standard test methods for in situ measurement of masonry mortar joint shear strength index’, C 1531 - 03, ASTM International, Pennsylvania, United States.

47 Rilem (1996). ‘MS-B.4 Determination of shear strength index for masonry unit/mortar junction’, *Materials and Structures*, **29**(8): 459-475.

48 Lourenço, P. B., Barros, J. O., Oliveira, J. T. (2004). ‘Shear testing of stack bonded masonry’, *Construction and Building Materials*, **18**(2): 125-132.

49 Institute of Statistics and Mathematics (2010). ‘The R project for statistical computing’, *Institute of Statistics and Mathematics*, Vienna, Austria.

50 Peck, R., Olsen, C., Devore, J. L. (2009). ‘Introduction to statistics and data analysis’, Brooks/Cole, Cengage Learning, Belmont, California, United States.

51 Chi, Y. (2014). ‘R-tutorial, an R introduction to statistics’, http://www.r-tutor.com/elementary-statistics/non-parametric-methods/kruskal-wallis-test.

52 Oakdale Engineering (2010). ‘DataFit 9.0’, Oakdale Engineering, Oakdale, United States. http://www.oakdaleengr.com/.

APPENDIX A: MATERIAL PROPERTIES DATA SET

Whilst recognising the limitations of providing material property test results without accompanying illustrations of the appearance of the associated test samples, the data set presented in this appendix is provided for the purpose of demonstrating characteristic properties for clay brick URM buildings of different ages and locations from throughout New Zealand. The data has been obtained based on permissible circumstances at each building site, and hence different tests were conducted for different sites and differing numbers of samples were collected and tested. Samples from Christchurch were principally sourced from earthquake-damaged buildings scheduled for demolition, whereas data from other located derived from both buildings that were being investigated as part of detailed seismic assessment and improvement, and buildings scheduled for demolition.

Table A1 reports the general location and building age, where known, as also shown in Figure 9. The raw data reported in Table A2 is presented as a resource for engineers to see typical variations between properties within a building, variation in properties between buildings from similar parts of New Zealand and built at similar times, and as a potential resource for future researchers.

Table A1: Details of Field Sites

Building #	Address/name	City	Year built	Building #	Address	City	Year built
1	13 Gore Street	Auckland	-	**40**	HB	Auckland	1940's
2	24 Princess Street	Auckland	1882	**41**	Corner Ward and Anglesea Streets	Hamilton	1917
3	292 Cashel Street	Christchurch	-	**42**	H	Auckland	2009
4	311 Manakau Road	Auckland	1924	**43**	75 Victoria Street West	Auckland	1886
5	317 New North Road	Auckland	-	**44**	133 Franklin Road	Auckland	1886
6	CPIT F-Block	Auckland	-	**45**	200 Madras Street	Christchurch	-
7	Windsor Castle	Auckland	-	**46**	24 Main South Road	Christchurch	-
8	55 Customs Street	Auckland	-	**47**	689 Ferry Road	Christchurch	-
9	70 Jervois Road	Auckland	-	**48**	48 Idris road	Christchurch	-
10	2-6 Coles Crescent	Auckland	-	**49**	288b Lincoln Road	Christchurch	-
11	Textile building	Auckland	1908-1922	**50**	186 Ferry Road	Christchurch	-
12	UNITEC	Auckland	1865	**51**	58a Sandyford Street	Christchurch	-
13	1 Union Street	Auckland	1927	**52**	195 Armagh Street	Christchurch	-
14	144 Parnell Road	Auckland	1850	**53**	Te Kura Street	Christchurch	-
15	173 Sandringham Road	Auckland	Early 1900's	**54**	245-251 Ferry Road	Christchurch	-
16	2 Waverly Street	Auckland	1920	**55**	32 Armagh Street	Christchurch	-
17	286 Ponsonby Road	Auckland	1908	**56**	32 Armagh Street	Christchurch	-
18	9 Gore Street	Auckland	1915	**57**	46 Armagh Street	Christchurch	-
19	94 Queen Street	Auckland	1882	**58**	198 Madras Street	Christchurch	-
20	Alfred Nathan House	Auckland	1882	**59**	180 Tuam Street	Christchurch	-
21	Old Choral Hall	Auckland	1872	**60**	350 Lincoln Road	Christchurch	-
22	Waiuku War Memorial Hall	Auckland	1917	**61**	1 Wakefield Street	Christchurch	-
23	23 Shortland Street	Auckland	1905	**62**	51 Lichfield Street	Christchurch	-
24	38 Taupo Quay	Whanganui	Late 1910's	**63**	341 Cashel Street	Christchurch	-
25	42 Victoria Ave	Whanganui	-	**64**	301 Selwyn Street	Christchurch	-
26	165-167 Ponsonby Road	Auckland	1922	**65**	24 Union Street	Christchurch	-
27	203 Hobson Street	Auckland	1911	**66**	273 Montreal Street	Christchurch	-
28	7 Sales Street	Auckland	1920	**67**	194 Hereford Street	Christchurch	-
29	476 Mt Eden Road	Auckland	1915	**68**	4 Donald Street	Christchurch	-
30	2-6 Todd Plaza	Auckland	Early 1900's	**69**	London Streets	Christchurch	-
31	44 Wallace Street	Wellington	1884	**70**	Oxford Street	Christchurch	-
32	30 Whitaker Place	Auckland	1913	**71**	42 London Street	Christchurch	-
33	57 Customhouse Street	Gisborne	1907	**72**	44 London Street	Christchurch	-
34	64 Customhouse Street, Gisborne	Gisborne	1906	**73**	1 Sumner Road	Christchurch	-
35	203-271 Victoria Street West	Auckland	1910	**74**	382-406 Colombo Street	Christchurch	-
36	107 Dominion Road	Auckland	1940s	**75**	437 Colombo Street	Christchurch	-
37	624 Te Rahu Road	Te Awamutu	-	**76**	14 Bedford Road	Christchurch	-
38	3176 Great North Road, New Lynn	Auckland	1880s	**77**	239 Manchester Street	Christchurch	-
39	29 Great North Road	Auckland	1930s	**78**	135 Kilmore Street	Christchurch	-

Continued Table A1: Details of Field Sites

Building #	Address/name	City	Year built
79	305 Manchester Street	Christchurch	-
80	866 Colombo Street	Christchurch	-
81	227 Manchester Street	Christchurch	-
82	143 Worcester Street	Christchurch	-
83	203 Hereford Street	Christchurch	-
84	156 Gloucester Street	Christchurch	-
85	1047 Colombo Street	Christchurch	-
86	40 Phillips Street	Christchurch	-
87	94 Gloucester Street	Christchurch	-
88	25 Armagh Street	Christchurch	-
89	3 Aynsley Tce	Christchurch	-
90	789 Colombo Street	Christchurch	-
91	124-126 Cashel Street	Christchurch	-
92	237 Cambridge Tce	Christchurch	-
93	17 Winchester Street	Christchurch	-
94	1 Papanui Road	Christchurch	-
95	85 Lambton Quay	Wellington	1881
96	AUST	-	-
97	49 Victoria Road, Devonport	Auckland	Early 1900s
98	AUW	-	-

Table A2: Raw Data

Building #	f'_b (MPa)	f'_i (MPa)	c (MPa)	Building #	f'_b (MPa)	f'_i (MPa)	c (MPa)	Building #	f'_b (MPa)	f'_i (MPa)	c (MPa)
1	21.31	3.94	1.07	**9**	13.36	2.62	0.27	**18**	11.58	1.70	0.95
	14.19	5.71	0.99		13.96	2.88	0.62		18.02	1.99	0.92
	19.77	0.73	0.20		16.34	3.90	0.51		15.22	2.73	1.35
	14.93	0.70	0.32	**10**	10.67	1.18	0.35		16.27	0.65	0.45
	26.30	5.10	1.50		11.35	1.52	0.26	**19**	8.80	4.20	0.65
	12.20	3.90	0.98		9.42	2.41	0.21		24.70	3.60	0.28
	13.86	4.20	1.15		11.85	1.72	0.47		8.70	6.00	0.69
	11.21	4.50	0.96		12.28	2.23	0.45	**20**	11.58	2.56	1.07
	15.94	1.30	0.38	**11**	31.89	4.13	1.19		10.20	2.76	1.05
	16.53	0.90	0.90		28.50	3.95	1.14		8.16	2.34	0.82
	42.92	2.30	0.83		14.54	2.79	1.23		9.68	3.10	0.94
	30.03	1.60	0.67		23.72	3.60	1.15		11.47	1.80	0.82
2	13.09	2.97	1.36		14.39	3.00	1.12		8.40	1.70	0.57
	12.02	3.23	1.39		15.11	4.01	1.12		12.77	1.60	0.84
	11.86	2.75	0.92	**12**	18.03	3.86	0.28		11.54	1.50	0.51
	11.87	3.42	1.09		17.92	0.72	0.34		8.55	2.50	0.63
	13.40	2.32	0.95		12.48	3.25	0.85		7.78	2.50	0.45
	11.04	2.15	0.57		19.64	2.15	0.51	**21**	24.99	6.69	1.04
	15.10	2.14	0.93		16.43	6.78	0.86		25.43	2.56	0.72
	12.23	1.81	0.54		13.85	5.37	0.81		23.53	1.71	1.13
	11.43	3.12	0.70		33.46	3.11	0.26		24.72	1.02	1.53
	9.75	2.74	0.45		20.40	3.66	1.00		12.24	0.88	0.33
3	23.73	10.99	0.83		13.35	0.21	0.23		28.49	0.97	0.70
	45.09	12.47	0.91		24.54	1.09	0.11		26.89	1.04	0.50
	15.32	8.74	1.18		38.37	4.92	1.02		32.69	1.63	0.27
	16.98	8.10	0.58		13.30	4.03	0.98		30.34	2.37	0.42
4	21.80	4.00	1.48		15.67	3.20	0.27		21.22	1.21	0.31
	14.80	5.00	0.82		13.00	0.92	0.12		24.00	1.79	0.42
	19.20	2.30	0.90		15.04	2.69	1.04		19.29	0.97	0.25
	13.30	5.60	1.52		12.91	0.25	0.11		28.27	4.19	0.48
5	24.83	5.30	1.37	**13**	10.01	1.49	0.69	**22**	45.68	2.77	0.54
	24.44	4.92	1.23		11.65	1.95	0.63		30.67	2.71	0.90
	11.43	4.85	1.06		6.79	3.00	1.00		30.15	5.29	0.95
	18.87	4.10	0.64		6.62	2.54	1.22		26.17	2.68	0.88
	11.22	6.00	0.96	**14**	17.50	0.40	0.12		23.96	2.87	0.59
	29.14	4.40	1.01		15.59	0.43	0.12		31.74	2.78	0.67
6	40.57	2.72	0.96	**15**	11.35	1.18	0.47		41.04	3.15	0.47
	15.98	6.03	0.78		14.76	1.24	0.43		41.55	1.49	0.97
	21.56	1.77	0.36	**16**	46.90	3.60	0.70	**23**	14.90	1.00	0.70
	16.18	3.63	0.73		35.40	3.70	0.92		25.00	1.40	0.66
7	17.50	0.40	0.12		26.70	3.10	0.67	**24**	26.70	1.20	0.61
	15.59	0.43	0.12		18.10	0.75	0.37		37.50	2.10	0.25
8	17.00	1.83	0.80	**17**	12.01	0.97	0.33	**25**	29.20	1.20	0.18
	21.73	2.79	0.60		12.87	1.63	0.28		20.80	0.70	0.43
					12.18	1.17	0.31		16.70	1.40	0.33
					10.75	2.69	0.70				

Continued Table A2: Raw Data

Building #	f'_b (MPa)	Moh's Hardness	f'_j (MPa)	Moh's Hardness	c (MPa)	MoR (MPa)	f'_m (MPa)	E'_m (MPa)	f'_{fb} (MPa)
26	21.59		2.60		0.89				
	30.01		0.73		0.39				
27	22.00		1.95		0.42				
	16.09		3.46		0.93				
	14.72		2.76		0.52				
	19.51		2.50		0.31				
	30.90		3.20		0.31				
	27.91		1.50		0.34				
28	17.40		3.40		1.23				
	17.90		2.90		0.68				
	26.70		5.40		0.63				
29	9.05		6.94		0.63				
	22.41		3.06		0.53				
	38.00		4.85		0.77				
	14.44		3.40		0.65				
30	17.83		3.17		0.37				
	19.07		2.80		0.35				
31	11.00	2.5	1.28	1.5	0.12	1.1	2.25	282	0.036
	8.80	2.5	1.24	1.5	0.24	1.6	3.92	518	0.040
	6.50	2.5	1.31	1.5	0.55	1.5	3.50	455	0.027
	6.40	2.5	1.61	1.5	0.45	1.1	3.63	299	0.020
	9.40	2.5	1.03	1.5	0.16	0.7			0.031
	6.50	2.5	1.11	1.5	0.15				0.024
	10.30	2.5	1.00	1.5					0.041
	9.90	2.5	0.69						
	11.00	2.5	2.47						
	9.50	2.5	4.95						
	11.70	2.5	8.65						
	11.90	2.5	2.10						
	8.10	2.5	1.23						
	8.50	2.5	4.14						
	12.90		8.58						
	13.10		5.92						
	10.10		6.65						
	8.60								
	12.40								
32	11.50	2.5				1.7			
	9.90	2.5				1.4			
	14.50	2.5				1.8			
	7.50	2.5				1			
	14.80	2.5				1			
	15.30	2.5				1.3			
	9.10	2.5				2.2			
	10.20	2.5				1.9			
	13.10	2.5							
	12.90	2.5							
	19.20	2.5							
	16.00	2.5							
	13.30	2.5							
	10.10	2.5							
	9.00	2.5							
	5.70	2.5							
	9.40	2.5							
	7.20	2.5							
	11.50								
	12.80								
	9.90								
	12.60								
	7.60								
	12.40								
	19.50								
	10.70								
33	16.90	2.5							
	15.40	2.5							
	11.40	2.5							
	14.60	2.5							

Building #	f'b (MPa)	Moh's Hardness	f'i (MPa)	Moh's Hardness	c (MPa)	MoR (MPa)	f'm (MPa)	E'm (MPa)	f'fb (MPa)
	15.90	2.5							
	11.20	2.5							
	10.90	2.5							
	8.70	2.5							
	15.10	2.5							
	10.20	2.5							
	17.40	2.5							
34	13.00	2.5	5.02	1.5		2.2	12.12	2401	
	14.20	2.5	6.86	1.5		1.3	10.11	2443	
	11.50	2.5	6.22	1.5		1.4	10.26	1809	
	11.80	2.5	4.38	2.0		1.3	11.04	1877	
	12.30	2.5	6.48	2.0		2.1			
	15.30	2.5	4.27	2.0		2.1			
	21.30	2.5	4.91	2.5		1.8			
	19.10	2.5	6.07	2.5		2.1			
	23.50	2.5				2.5			
	12.80	2.5							
	20.20	2.5							
	17.20	2.5							
	8.10	2.5							
	11.70	2.5							
	15.30	2.5							
	12.40	2.5							
	10.50	2.5							
	18.20	3.0							
	15.20								
	17.80								
	16.00								
	12.90								
	15.10								
	12.80								
	20.20								
	17.20								
	11.70								
35	21.10	3.0	2.86	2.0		2.2	8.26	2475	0.142
	15.60	3.0	3.42	2.0		3.1	6.70	1879	0.122
	14.20	3.0	4.11	2.0	0.24	2.8	8.06	1756	0.095
	14.80	3.0	3.91	2.0		3.6	8.04	1336	0.106
	21.70	3.0	3.29	2.0					
	15.80	3.0	3.78	2.0					
	17.80	3.0	5.05	2.0					
	23.80	3.0	3.37	2.0					
	22.20	3.0	4.72	2.0					
	15.00	3.0	4.85	2.0					
	26.30	3.0	4.25	2.5					
	19.60	2.5	3.95	2.5					
	15.80	2.5	4.95	2.0					
	17.80	2.5	5.41	2.0					
	14.00	2.5							
	21.70	3.0							
	21.00	3.0							
	20.30	3.0							
	15.60								
	21.70								
	23.80								
	26.30								
36	20.20	2.5	3.58	2.0		2	6.36	1239	0.050
	19.50	2.5	2.07	2.0		1.5	5.35	2015	0.063
	18.80	2.5	2.13	2.0		3.2	5.29	1555	0.058
	16.10	2.5	2.40	2.0		3.1	7.25	1159	
	29.80	2.5	2.56	2.0		3			
	12.50		2.19	2.0		2			
	10.50		2.54	2.0		3.3			
	19.90		2.77	2.0		3.5			
	16.70		2.17	2.0		2.7			
	16.40		2.33	2.0		2			
	22.00		2.44	2.0		2.1			

Building #	f'_b (MPa)	Moh's Hardness	f'_i (MPa)	Moh's Hardness	c (MPa)	MoR (MPa)	f'_m (MPa)	E'_m (MPa)	f'_{fb} (MPa)
	21.60		2.02	2.0					
	20.20		2.98	2.0					
	19.50		3.08	2.0					
	18.80		3.60	2.0					
	16.10		3.00	2.0					
37	23.00	2.5	6.79	2.0			12.85	4573	0.094
	15.70	2.5	6.60	2.0			13.11	4471	0.126
	26.80	2.5	4.25	2.0			12.85	3939	0.140
	19.20	2.5	5.53	2.0	0.33		12.54	3846	0.095
	24.20	2.5	4.83	2.0			12.05	3382	0.179
	12.30	2.5	6.15	2.5			13.11	3809	
	24.10	2.5	7.09	2.0					
	24.90	2.5	6.13	2.5					
	19.50	2.5							
38	22.50	4.0				2.5			
	12.80	2.5				2.7			
	27.70	2.5				2.5			
	25.00	2.5				2.4			
	8.90	2.5				4.5			
	10.40	2.5				1.5			
	14.30	2.5							
	16.20	2.5							
	31.80	3.0							
	35.50	3.0							
	34.90	3.0							
	29.80	3.0							
	37.70	3.0							
	26.60	3.0							
	22.80	3.0							
	26.90	3.0							
	29.90	3.0							
	45.80	3.0							
	27.70								
	29.90								
	25.00								
	29.80								
	35.50								
	16.20								
39	26.60	2.5	9.33	2.5		3.3	14.16	3120	0.140
	19.90	2.5	7.72	2.5		3.6	13.09	3831	0.134
	30.00	2.5	6.07	2.5		4.9	15.75	3695	0.206
	27.70	2.5	7.66	2.0		4	17.47	5399	0.236
	22.80	3.0	6.93	2.0		3.8	15.10	5387	0.151
	27.70	3.0	6.47	2.5	0.39	3.7			0.162
	24.90	3.0	5.14	2.5		3.1			
	28.70		5.39	2.5		3.9			
	30.80		5.07	2.5					
	33.60		6.77	2.5					
	35.80		6.61	2.5					
	25.90								
	26.40								
	19.90								
	30.00								
40	28.30	3.0							
	27.50	3.0							
	42.20	3.0							
	34.30	3.0							
	32.10	3.0							
	32.50	3.0							
	41.00	3.0							
	31.90	3.0							
	34.70	3.0							
	32.50	3.0							
	41.00	3.0							
	31.90	3.0							
	34.70	3.0							
41	29.40	4.0							

Building #	f'$_b$ (MPa)	Moh's Hardness	f'$_i$ (MPa)	Moh's Hardness	c (MPa)	MoR (MPa)	f'$_m$ (MPa)	E'$_m$ (MPa)	f'$_{fb}$ (MPa)
	40.90	4.0							
	42.90	4.0							
	26.10	4.0							
	38.10	4.0							
	31.30	4.0							
	22.10	4.0							
	44.10	4.0							
	44.10	4.0							
	30.60	4.0							
	24.20	4.0							
	35.40	4.0							
	34.10	4.0							
	38.30	4.0							
	34.60	4.0							
42	35.80	4.0							
	28.30	4.0							
	32.70	4.0							
	39.60	4.0							
	38.80	4.0							
	39.80	4.0							
	41.50	4.0							
	37.20	4.0							
	40.20	4.0							
	45.10	4.0							
	52.10	4.0							
43	6.20					0.7			
	11.90					1.4			
	6.80					0.5			
	13.40					1.4			
	13.30					1			
	10.50					0.9			
	8.00					0.6			
44			4.06	2.0			8.33	2129	
			3.83	2.0			10.01	3394	
			4.55	2.0			7.43	1876	
			4.97	2.0			5.94	1565	
			5.38	2.5			6.23	2296	
			4.44	2.5					
45			2.70	2.0					
			3.02	1.5					
			2.13	1.5					
46			0.94	1.5					
			1.14	1.5					
			0.83	1.5					
			1.15	1.5					
47			0.80	1.5					
			0.86	1.5					
			0.66	1.5					
			0.54	1.5					
			0.56	1.5					
			0.51	1.5					
48			0.85	1.5					
			1.22	1.5					
			0.81	1.5					
			1.34	1.5					
			1.16	1.5					
49			0.47	1.5					
			0.37	1.5					
			0.66	1.5					
			0.61	1.5					
50			0.80	1.5					
			1.60	1.5					
			1.99	1.5					
			1.34	1.5					
			1.57	1.5					
			2.04	1.5					
51			1.18	1.5					

Building #	f'_b (MPa)	Moh's Hardness	f'_i (MPa)	Moh's Hardness	c (MPa)	MoR (MPa)	f'_m (MPa)	E'_m (MPa)	f'_{fb} (MPa)
			0.73	1.5					
			1.15	1.5					
			1.09	1.5					
			1.21	1.5					
52			1.99	1.5					
			0.94	1.5					
			1.09	1.5					
			1.62	1.5					
			1.61	1.5					
53			0.92	1.5					
			1.29	1.5					
			1.18	1.5					
			1.10	2.0					
			1.43	2.0					
54			0.85	1.5					
			1.41	1.5					
			0.88	1.5					
			1.20	1.5					
			0.78	1.5					
			1.04	1.5					
55			0.80	1.5					
			1.04	1.5					
			1.19	1.5					
56			3.21	2.0					
			2.58	2.0					
			2.89	2.0					
			2.51	2.0					
57			0.67	1.5					
			0.74	1.5					
			0.60	1.5					
			1.03	2.0					
58			1.12	1.5					
			1.22	1.5					
			1.38	1.5					
			1.12	1.5					
59			3.94	2.0					
			2.74	2.0					
			3.32	2.0					
			3.57	2.0					
60			1.89	1.5					
			1.16	1.5					
			1.12	1.5					
61			1.88	2.0					
			2.75	2.0					
			2.86	2.0					
			2.32	2.0					
62			2.08	1.5					
			2.25	1.5					
			2.20	1.5					
			2.65	2.0					
63			4.03	2.0					
			7.95	2.0					
			6.37	2.0					
64			2.48	1.5					
			2.46	1.5					
			2.63	1.5					
			3.00	1.5					
65			0.98	1.5					
			0.98	1.5					
			1.19	1.5					
66			1.43	1.5					
			1.35	1.5					
			0.98	1.5					
			1.08	1.5					
67			4.13	2.0					
			3.31	2.0					

Building #	f'$_b$ (MPa)	Moh's Hardness	f'$_i$ (MPa)	Moh's Hardness	c (MPa)	MoR (MPa)	f'$_m$ (MPa)	E'$_m$ (MPa)	f'$_{fb}$ (MPa)
			4.00	1.5					
			3.83	2.0					
68			0.85	1.5					
			1.08	1.5					
			1.44	1.5					
			1.10	1.5					
			1.09	1.5					
69			6.20	2.0					
			6.79	2.0					
			5.69	2.0					
			9.34	2.5					
70			0.71	1.5					
			1.00	1.5					
			0.80	1.5					
			1.12	1.5					
			0.86	1.5					
71			1.79	1.5					
			2.49	1.5					
			3.22	1.5					
			2.61	1.5					
			2.82	1.5					
72			0.99	1.5					
			0.74	1.5					
			0.83	1.5					
			0.87	1.5					
73			0.86	1.5					
			0.74	1.5					
			0.99	1.5					
			0.82	1.5					
			0.59	1.5					
74			3.99	2.0					
			3.89	2.0					
			3.11	2.0					
			3.69	2.0					
			4.09	2.0					
			3.12	2.0					
75			1.18	1.5					
			0.81	1.5					
			0.85	1.5					
			0.95	1.5					
			0.73	1.5					
			1.10	1.5					
76			2.09	1.5					
			2.10	1.5					
			2.27	1.5					
			2.59	1.5					
			2.68	1.5					
			2.57	1.5					
77			1.01	1.5					
			0.89	1.5					
			1.20	1.5					
			0.77	1.5					
			0.72	1.5					
			1.09	1.5					
			0.87	1.5					
78			3.23	1.5					
			2.69	1.5					
			3.31	1.5					
			2.44	1.5					
79			1.37	1.5					
			1.84	1.5					
			1.78	1.5					
			1.43	1.5					
			1.31	1.5					
			1.58	1.5					
80			4.20	2.0					
			2.76	2.0					

Building #	f'$_b$ (MPa)	Moh's Hardness	f'$_i$ (MPa)	Moh's Hardness	c (MPa)	MoR (MPa)	f'$_m$ (MPa)	E'$_m$ (MPa)	f'$_{fb}$ (MPa)
			3.82	2.0					
			3.50	2.0					
81			2.34	2.0					
			2.67	2.0					
			2.64	2.0					
			2.44	2.0					
82			0.74	1.5					
			0.81	1.5					
			0.97	1.5					
			1.33	1.5					
83			16.62	3.0					
				3.0					
			14.79	3.0					
84			2.61	2.5					
			2.17	2.0					
			2.87	2.0					
			2.46	2.0					
			2.56	2.0					
			2.12	2.0					
85			1.95	1.5					
			1.34	1.5					
			1.86	1.5					
			1.66	1.5					
			1.32	1.5					
			1.76	1.5					
			1.83	1.5					
			1.79	1.5					
86			0.90	1.5					
			0.92	1.5					
			0.85	1.5					
			0.90	1.5					
			0.98	1.5					
			1.07	1.5					
87			1.58	1.5					
			1.80	1.5					
			1.89	1.5					
			0.89	1.5					
			2.00	1.5					
			0.95	1.5					
			1.39	1.5					
88			0.73	1.5					
			0.55	1.5					
			0.47	1.5					
			0.58	1.5					
			0.44	1.5					
			1.12	1.5					
			1.24	1.5					
			1.22	1.5					
			1.26	1.5					
			1.10	1.5					
			1.18	1.5					
89			0.77	1.5					
			0.57	1.5					
			0.84	1.5					
			0.79	1.5					
90			0.82	1.5					
			0.87	1.5					
			0.81	1.5					
91			8.17	2.5					
			10.71	2.5					
			11.71	2.5					
			13.42	2.5					
92			2.83	2.0					
			3.32	2.0					
			4.64	2.0					
			4.66	2.5					
			3.64	2.5					

Building #	f'$_b$ (MPa)	Moh's Hardness	f'$_i$ (MPa)	Moh's Hardness	c (MPa)	MoR (MPa)	f'$_m$ (MPa)	E'$_m$ (MPa)	f'$_{fb}$ (MPa)
			3.71	2.5					
			5.13	2.5					
93			1.60	1.5					
			1.08	1.5					
			0.83	1.5					
			1.20	1.5					
			1.12	1.5					
			0.87	1.5					
94			0.87	1.5					
			1.11	1.5					
			0.92	1.5					
			1.09	1.5					
			1.49	1.5					
			0.81	1.5					
			1.11	1.5					
95			10.30	2.5			6.31	1574	0.287
			8.09	2.5			7.30	1559	0.316
			9.50	2.5			5.64	1504	0.457
			9.41	2.5			5.70	2057	0.285
			8.99	2.5			9.37	3121	0.380
			10.33	2.5					
			7.88	2.5					
			8.61	2.5					
			9.04	2.5					
			6.78	2.0	0.43				
			7.30	2.5					
			6.89	2.5					
			7.20	2.5					
			10.00	2.5					
			9.07	2.5					
			7.85	2.5					
96			1.06	1.5					
			0.93	1.5					
			0.89	1.5					
			1.07	1.5					
			0.90	1.5					
			1.21	1.5					
			1.04	1.5					
			1.14	1.5					
			1.32	1.5					
			1.51	1.5					
			1.93	1.5					
			1.44	1.5					
			1.12	1.5					
			1.15	1.5					
			1.21	1.5					
			1.46	1.5					
97			1.59	1.5					
			1.35	1.5					
			1.95	1.5					
			1.51	1.5					
			1.68	1.5					
98			1.00	1.5					
			0.68	1.5					
			0.73	1.5					
			0.57	1.5					
			0.64	1.5					
			0.89	1.5					
			0.74	1.5					
			0.65	1.5					